Models for Steric Interactions in Heme Proteins. Structures of the Five-Coordinate Complex Iron(III) Tetraphenylporphyrin Azide and Its Six-Coordinate 1:1 Adducts with 1-Methylimidazole and 1,2-Dimethylimidazole

Y. Zhang,[†] W. A. Hallows,[†] W. J. Ryan,[†] J. G. Jones,[‡] G. B. Carpenter,[†] and D. A. Sweigart[*],[†]

Department of Chemistry, Brown University, Providence, Rhode Island 02912, and Department of Applied Physical Sciences, University of Ulster, Coleraine BT52 1SA, U.K.

A structural study of the high-spin five-coordinate complex iron(III) tetraphenylporphyrin azide Fe(TPP)N$_3$ (**3**) and its six-coordinate low-spin adducts with 1-methylimidazole (1-MeIm) and 1,2-dimethylimidazole (1,2-Me$_2$Im) is presented. The latter two complexes were studied in order to explore the structural effect of steric strain induced by the presence of the 2-methyl substituent and to determine to what extent, if any, the set of complexes Fe-(TPP)(1-MeIm)N$_3$ (**4**) and Fe(TPP)(1,2-Me$_2$Im)N$_3$ (**5**) mimic the structural differences observed in the vicinity of the metal in R-state HbO$_2$ and T-state HbO$_2$, respectively. Crystal data for **3**: triclinic space group $P\bar{1}$, $a = 11.214(5)$ Å, $b = 12.623(6)$ Å, $c = 14.289(6)$ Å, $\alpha = 82.36(4)°$, $\beta = 68.78(3)°$, $\gamma = 66.72(3)°$, $Z = 2$, 4119 unique reflections, $R = 0.066$. Crystal data for **4**: monoclinic space group $P2_1/n$, $a = 12.758(6)$ Å, $b = 24.273(6)$ Å, $c = 14.755(7)$ Å, $\beta = 106.42(3)°$, $Z = 4$, 3553 unique reflections, $R = 0.086$. Crystal data for **5**: monoclinic space group $P2_1/n$, $a = 13.045(4)$ Å, $b = 24.059(29)$ Å, $c = 14.694(5)$ Å, $\beta = 103.88(2)°$, $Z = 4$, 3710 unique reflections, $R = 0.094$. The azide ligand in **3**–**5** is bonded in a bent fashion with a Fe–N–N angle of 122°. The porphyrin core in **3** is domed with the iron displaced 0.46 Å from the plane of the four pyrrole nitrogens (P$_N$). In **4** and **5** the porphyrin core displays approximate S_4 ruffling with the metal located nearly in the P$_N$ plane. In going from **4** to **5** there is essentially *no change* in the Fe–N$_3$ or Fe–N$_p$ (pyrrole nitrogen) bond distances. However, steric congestion is clearly manifested by (1) an increase of 0.083 Å in the Fe–N$_{Im}$ bond distance and (2) a tipping of the imidazole ligand in **5** by about 15° from the symmetrical position observed in **4**. These results and others are compared to the structural features of the analogous picket fence complexes Fe(TpivPP)(RIm)O$_2$ (RIm = 1-MeIm and 2-MeIm) and are discussed with reference to possible structural changes that accompany the T-HbO$_2$ to R-HbO$_2$ switch.

Introduction

In T-state deoxyhemoglobin (deoxy-Hb) it is thought that movement of the iron into the porphyrin plane upon binding of an axial ligand such as oxygen is inhibited by steric constraints in the vicinity of the heme.[1] In the resulting T-state HbO$_2$, these steric interactions are evidenced by a variety of structural features: doming of the porphyrin core, tilting of the F8-proximal imidazole ring, and relatively long bonds from the metal to the imidazole and oxygen axial ligands. Upon conversion to the R-state conformation of HbO$_2$, it appears[1] that the core doming and imidazole tilt vanish with a concomitant movement of the metal closer to the heme plane, resulting in stronger bonding to both axial ligands. This behavior is mimicked to some extent by the picket fence hemes Fe(TpivPP)(1-MeIm)O$_2$ (**1**) and Fe-(TpivPP)(2-MeIm)O$_2$ (**2**).[2,3] X-ray structures of **1** and **2** indicate end-on binding of O$_2$ to the iron with a Fe–O–O bond angle of ca. 130°. It was shown that **1** and **2** possess some structural features consistent with R-HbO$_2$ and T-HbO$_2$, respectively. In particular, the change **2** → **1** is accompanied by some movement of the iron toward the heme plane, untilting of the imidazole, and a large decrease of 0.153(25) Å in the Fe–O$_2$ bond length. Curiously, the iron–imidazole (Fe–N$_{Im}$) bond length changes relatively little (0.039(22) Å). Unfortunately, the structure determinations of **1** and **2** were plagued by disorder in the O$_2$

ligand. With **1**, there was additional disorder and high thermal motion in other parts of the molecule (including the 1-MeIm ligand); this, along with a small data set, placed severe limits on the structural precision.

Some years ago, during the course of kinetics studies, we had occasion to synthesize the set of complexes Fe(TPP)N$_3$ (**3**), Fe(TPP)(1-MeIm)N$_3$ (**4**), and Fe(TPP)(1,2-Me$_2$Im)N$_3$ (**5**). The azide ligand in **3**–**5** is bonded to the metal in a bent fashion (*vide infra*), as is also the case in met-HbN$_3$.[4] Azide binding to met-Hb is in some ways structurally analogous to oxygen binding to Hb,[4] especially if HbO$_2$ is viewed as having a superoxide ligand. Accordingly, it occurred to us that **4** and **5** may display steric interactions that model those in R- and T-HbO$_2$. Herein we report the X-ray structure of **3**–**5** and show that the steric strain in **5** induced by the 2-Me substituent leads to an elongated Fe–N$_{Im}$ bond and imidazole ring tipping (*vide infra*), both of which are alleviated upon going to **4**. Interestingly, the steric demands of the 1,2-Me$_2$Im ligand in **5** do *not* produce an increased Fe–N$_3$ bond length over that in **4**. This contrasts with the reported[2,3] much longer Fe–O$_2$ bond in **2** in comparison to that in **1**.

Experimental Section

Fe(TPP)N$_3$ (**3**) was synthesized as previously reported.[5] The six-coordinate imidazole adducts of **3** have been characterized in solution in previous work.[5,6] For X-ray and magnetic susceptibility measurements, complexes **3**–**5** were isolated as solids by slow crystallization as described

(1) (a) Perutz, M. F.; Fermi, G.; Luisi, B.; Shaanan, B.; Liddington, R. C. *Acc. Chem. Res.* **1987**, *20*, 309. (b) Liddington, R.; Derewenda, Z.; Dodson, G.; Harris, D. *Nature* **1988**, *331*, 725. (c) Perutz, M. F. *Adv. Exp. Med. Biol.* **1982**, *148*, 31.
(2) Jameson, G. B.; Rodley, G. A.; Robinson, W. T.; Gagne, R. R.; Reed, C. A.; Collman, J. P. *Inorg. Chem.* **1978**, *17*, 850.
(3) Jameson, G. B.; Molinaro, F. S.; Ibers, J. A.; Collman, J. P.; Brauman, J. I.; Rose, E.; Suslick, K. S. *J. Am. Chem. Soc.* **1980**, *102*, 3224.

(4) (a) Deatherage, J. F.; Obendorf, S. K.; Moffat, K. *J. Mol. Biol.* **1979**, *134*, 419. (b) Moffat, K.; Deatherage, J. F.; Seybert, D. W. *Science* **1979**, *206*, 1035.
(5) Byers, W.; Cossham, J. A.; Edwards, J. O.; Gordon, A. T.; Jones, J. G.; Kenny, E. t. P.; Mahmood, A.; McKnight, J.; Sweigart, D. A.; Tondreau, G. A.; Wright, T. *Inorg. Chem.* **1986**, *25*, 4767.
(6) Adams, K. M.; Rasmussen, P. G.; Scheidt, W. R.; Hatano, K. *Inorg. Chem.* **1979**, *18*, 1892.

Table 1. Summary of Crystal Structure Data

	Fe(TPP)N₃	Fe(TPP)(1-MeIm)N₃	Fe(TPP)(1,2-MeIm)N₃
formula	$C_{44}H_{28}N_7Fe$	$C_{48}H_{34}N_9Fe$	$C_{49}H_{36}N_9Fe$
fw	710.60	792.70	806.73
space group	$P\bar{1}$, triclinic	$P2_1/n$, monoclinic	$P2_1/n$, monoclinic
crystal dimensions, mm	0.25 × 0.30 × 0.70	0.26 × 0.32 × 0.45	0.40 × 0.40 × 0.70
temperature, °C	20	20	20
a, Å	11.214(5)	12.758(6)	13.045(4)
b, Å	12.623(6)	24.273(6)	24.059(29)
c, Å	14.289(6)	14.755(7)	14.694(5)
α, deg	82.36(4)		
β, deg	68.78(3)	106.42(3)	103.88(2)
γ, deg	66.72(3)		
V, Å³	1732(1)	4383(2)	4477(5)
Z	2	4	4
ρ_{calcd}, g cm⁻³	1.36	1.20	1.20
radiation	Mo Kα, λ0.710 69 Å	Mo Kα	Mo Kα
μ, cm⁻¹	4.86	3.80	3.77
2θ limits, deg	3.5–45	3.5–45	3.5–40
no. of observns	4827	4652	4729
no. of unique data, $I > 1.0\sigma(I)$	4119	3553	3710
no. of variables	421	475	533
R^a	0.066	0.086	0.094
$R_w{}^b$	0.057	0.089	0.125
GOF	2.11	2.37	3.75

^{a} $R = \sum\lVert F_o\rvert - \lvert F_c\rVert/\sum\lvert F_o\rvert$. ^{b} $R_w = [\sum w(F_c - F_o)^2/\sum w(F_o)^2]^{1/2}$.

(3)

(4)   (5)
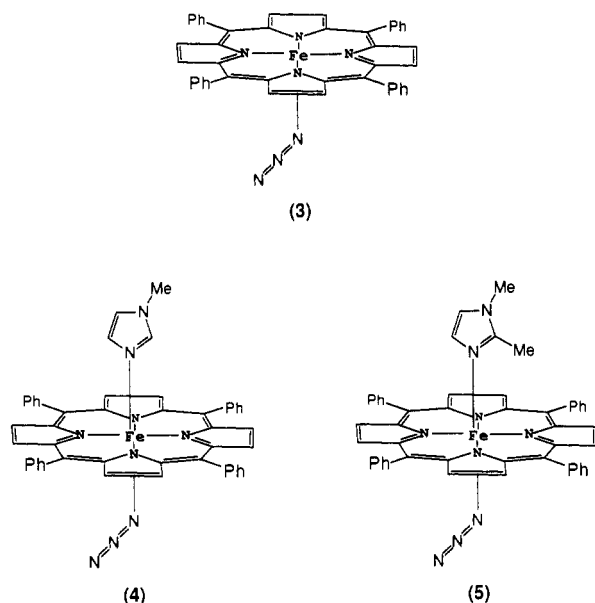
Figure 1. Complexes discussed in this study.

below. The molar magnetic susceptibility (χ_M) of **3** and **5** was measured by the Faraday method over the temperature range 77–293 K at a field strength of 10.4 k Oe. The field dependence of χ_M in the range 6.0–10.4 k Oe was determined at 77 and 193 K. Standard diamagnetic corrections were applied to all data. The crystalline samples of **3** and **5** used in the magnetic studies were carefully examined with a microscope before and after each experiment to verify the absence of impurities and/or decomposition.

X-ray Structure Determinations. Large dark blue opaque crystals of Fe(TPP)N₃ (**3**) were grown over 2–4 days by pentane vapor diffusion into a CH₂Cl₂ solution at 10 °C. A crystal was collected and glued to the end of a glass fiber. Twenty-three well-centered reflections were used to determine the cell dimensions, which proved to be triclinic. Standard θ–2θ data were collected at room temperature with a Nicolet R3m diffractometer. Azimuthal scans based on eight reflections well separated in reciprocal space were used for an empirical absorption correction. Analysis of the systematic absences showed the space group to be triclinic $P\bar{1}$. The structure was solved easily and quickly via direct methods using the SHELXTL 5.1 package.[7] All hydrogen atoms were placed in theoretical positions with a C–H bond length of 0.96 Å. The phenyl rings were constrained to regular hexagons (C–C bond length
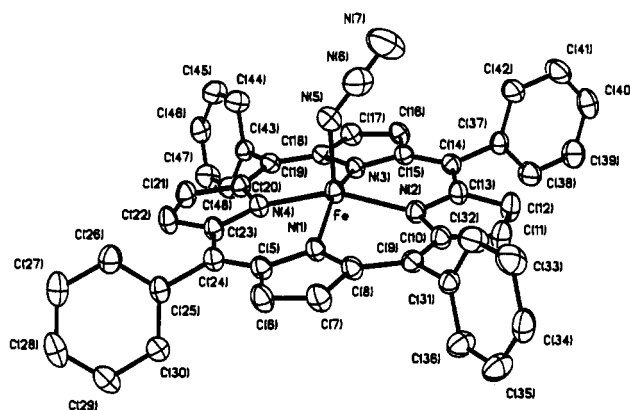
Figure 2. ORTEP diagram of Fe(TPP)N₃ (**3**). Probability surfaces are shown at 30%.

1.395 Å), and each refined as a rigid group. All non-hydrogen atoms were allowed to refine anisotropically with the weighting scheme $w = 1/[\sigma^2(F_o) + G(F_o)^2]$ ($G = 0.00010$).

Single crystals of Fe(TPP)(1-MeIm)N₃ (**4**) were grown by layering a CH₂Cl₂ solution containing equivalent amounts of Fe(TPP)N₃ and 1-MeIm with pentane in a 5 mm NMR tube at –18 °C. Crystal growth required about 10 days. A crystal was glued to a glass fiber and the unit cell dimensions were calculated from 11 well-centered reflections collected in the range $10° \leq 2\theta \leq 30°$. Data were collected in the standard θ–2θ format. Azimuthal scans based on 10 reflections were used for an empirical absorption correction. Analysis of systematic absences indicated the space group $P2_1/n$. The structure was solved by direct methods; the iron atom was identified from the initial electron density map, and all other non-hydrogen atoms were located from a series of successive difference Fourier maps. The phenyl groups were constrained to regular hexagons (C–C bond length 1.395 Å) and all hydrogens were placed in theoretical positions with a C–H bond length of 0.96 Å and with a thermal parameter equal to 1.2 times the equivalent isotropic value at the attached carbon. The G factor used in the weighting scheme was 0.00050. The slightly high values of R and R_w are attributed to the presence of a cluster of electron density peaks (maximum 1.10 e/Å³), which is *not* within van der Waals contact of the rest of the molecule. It is likely that some fractional solvent incorporation occurred, as is quite commonly seen with metalloporphyrins.[8]

Crystals of Fe(TPP)(1,2-Me₂Im)N₃ (**5**) were grown by pentane vapor diffusion into a CH₂Cl₂ solution of Fe(TPP)N₃ and 1,2-Me₂Im at –18 °C. A crystal was selected, cut to the size indicated in Table 1, and glued to a glass fiber. Data collection and refinement proceeded as above, except that the phenyl rings were allowed to refine freely. Hydrogen

(7) SHELXTL programs, Nicolet Instrument Co., Madison, WI.

(8) Scheidt, W. R.; Lee, Y. J. *Struct. Bonding* **1987**, *64*, 1.
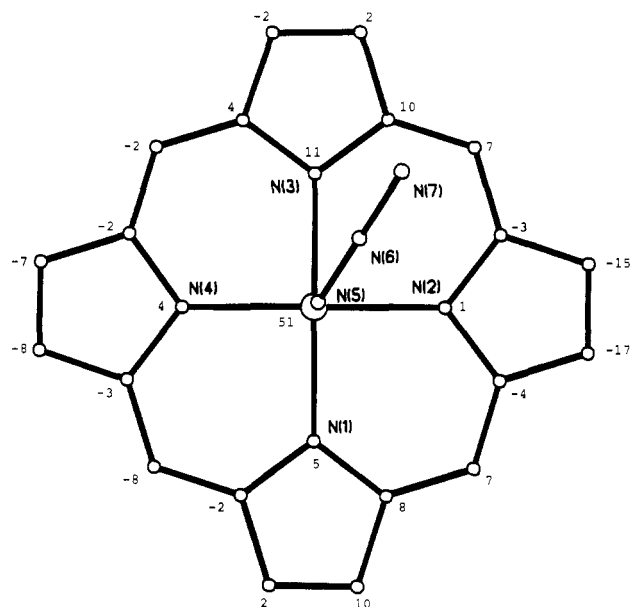
Figure 3. Diagram of the 24-atom porphyrin core in Fe(TPP)N₃ (3) showing displacements (in units of 0.01 Å) of each atom from the mean plane of the core.
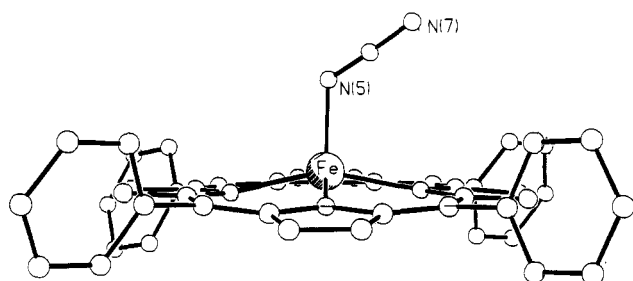
Figure 4. Side-on view of Fe(TPP)N₃ (3), showing the out-of-plane location of the iron and the angular disposition of the azide ligand.

atoms were placed in theoretical positions. The rather high R and R_w factors are due to the presence of a cluster of electron density (maximum 1.69 e/Å³), which is *not* within van der Waals contact of the porphyrin complex, that could not be identified. Attempts to model the cluster as free imidazole, pentane, or dichloromethane, were not successful. As noted above, partial incorporation of free solvent or ligand is not uncommon in metalloporphyrins, and this is most likely the case with the crystal of **5**.

Results and Discussion

Fe(TPP)N₃ (3) is a typical high-spin five-coordinate iron(III) porphyrin. Good adherence to the Curie law was found over the temperature range 77–293 K, with a temperature-independent effective magnetic moment, μ_{eff}, of 5.75(4) μ_B. This is close to the spin-only value expected for a d⁵ configuration with a ⁵A ground state. It is well-known[5,6,9,10] that Fe(TPP)X (X = F⁻, Cl⁻, N₃⁻) reacts with imidazoles (RIm) according to eqs 1 and 2. The Fe(TPP)(RIm)X species is high-spin for X⁻ = Cl⁻ and

$$Fe(TPP)X + RIm \rightarrow Fe(TPP)(RIm)X \qquad (1)$$

$$Fe(TPP)(RIm)X + RIm \rightarrow Fe(TPP)(RIm)_2{}^+X^- \qquad (2)$$
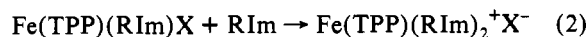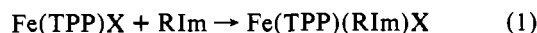
F⁻ and low-spin for X⁻ = N₃⁻. Generally eqs 1 and 2 occur very

(9) Walker, F. A.; Lo, M.-W.; Ree, M. T. *J. Am. Chem. Soc.* **1976**, *98*, 5552.
(10) (a) Burdige, D.; Sweigart, D. A. *Inorg. Chim. Acta* **1978**, *28*, L131. (b) Doeff, M. M.; Sweigart, D. A. *Inorg. Chem.* **1982**, *21*, 3699. (c) Tondreau, G. A.; Sweigart, D. A. *Inorg. Chem.* **1984**, *23*, 1060. (d) Jones, J. G.; Tondreau, G. A.; Edwards, J. O.; Sweigart, D. A. *Inorg. Chem.* **1985**, 24, 296. (e) Zhang, Y.; Jones, J. G.; Sweigart, D. A. *Inorg. Chim. Acta* **1989**, *166*, 85.

Table 2. Selected Atomic Coordinates (×10⁴) and Isotropic Thermal Parameters (Å² × 10³) for 3

	x	y	z	U_{eq}
Fe	4576(1)	6241(1)	2210(1)	44(1)
N(1)	6079(3)	4622(3)	1743(2)	45(2)
N(2)	4976(3)	6649(3)	712(2)	46(2)
N(3)	2648(3)	7545(3)	2483(2)	42(2)
N(4)	3701(3)	5470(3)	3494(2)	45(2)
C(5)	6400(4)	3677(3)	2348(3)	47(2)
C(6)	7721(4)	2845(4)	1812(3)	59(2)
C(7)	8194(4)	3272(3)	904(3)	58(2)
C(8)	7156(4)	4370(3)	844(3)	48(2)
C(9)	7216(4)	5066(3)	−7(3)	46(2)
C(10)	6160(4)	6094(3)	−72(3)	48(2)
C(11)	6178(5)	6751(4)	−972(3)	63(2)
C(12)	5034(5)	7728(4)	−733(3)	63(2)
C(13)	4279(4)	7682(3)	319(3)	48(2)
C(14)	3058(4)	8543(3)	862(3)	45(2)
C(15)	2292(4)	8460(3)	1857(3)	44(2)
C(16)	955(4)	9282(4)	2377(3)	54(2)
C(17)	505(4)	8860(3)	3296(3)	55(2)
C(18)	1555(4)	7779(3)	3376(3)	44(2)
C(19)	1448(4)	7065(3)	4205(3)	44(2)
C(20)	2457(4)	5998(4)	4252(3)	46(2)
C(21)	2365(4)	5261(4)	5104(3)	61(2)
C(22)	3504(4)	4291(4)	4874(3)	60(2)
C(23)	4345(4)	4399(3)	3865(3)	48(2)
C(24)	5588(4)	3553(3)	3323(3)	47(2)
N(5)	5512(3)	7021(3)	2615(3)	58(2)
N(6)	5237(4)	8029(4)	2519(3)	83(3)
N(7)	4992(6)	9038(5)	2431(4)	131(4)

Table 3. Selected Bond Lengths (Å) and Bond Angles (deg) for 3

Bond Lengths			
Fe–N(1)	2.071(3)	Fe–N(2)	2.060(3)
Fe–N(3)	2.070(3)	Fe–N(4)	2.063(3)
Fe–N(5)	1.953(5)	N(5)–N(6)	1.186(6)
N(6)–N(7)	1.192(8)		

Bond Angles			
N(1)–Fe–N(2)	86.9(1)	N(1)–Fe–N(3)	156.0(2)
N(2)–Fe–N(3)	87.4(1)	N(1)–Fe–N(4)	87.3(1)
N(2)–Fe–N(4)	152.8(2)	N(3)–Fe–N(4)	87.2(1)
N(1)–Fe–N(5)	103.9(1)	N(2)–Fe–N(5)	102.0(2)
N(3)–Fe–N(5)	100.1(1)	N(4)–Fe–N(5)	105.2(2)
Fe–N(5)–N(6)	121.8(4)	N(5)–N(6)–N(7)	178.1(7)
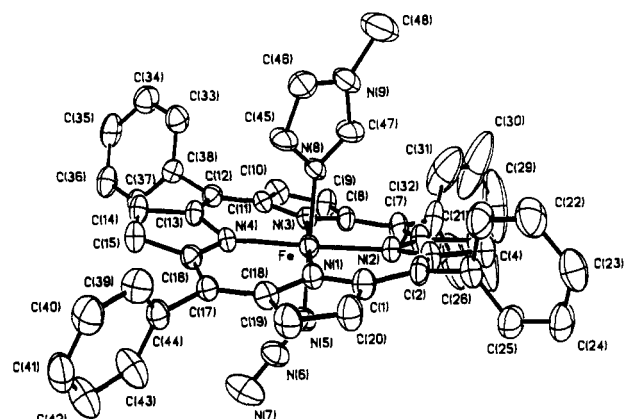
Figure 5. ORTEP diagram of Fe(TPP)(1-MeIm)N₃ (4). Probability surfaces are shown at 30%.

rapidly, with the result that Fe(TPP)(RIm)X can only be detected at low temperature. However, with X⁻ = N₃⁻, this species is more robust and can be prepared and studied at ambient temperature provided the imidazole is sterically congested (1,2-Me₂Im) or is replaced with a weak donor (e.g., pyridine).[6] We found that Fe(TPP)(1-MeIm)N₃ can also be prepared if an excess of 1-MeIm is avoided.

Scheidt et al. reported[6] the synthesis and structural characterization of Fe(TPP)(py)N₃. This complex is low-spin with a slightly temperature-dependent magnetic moment ranging from
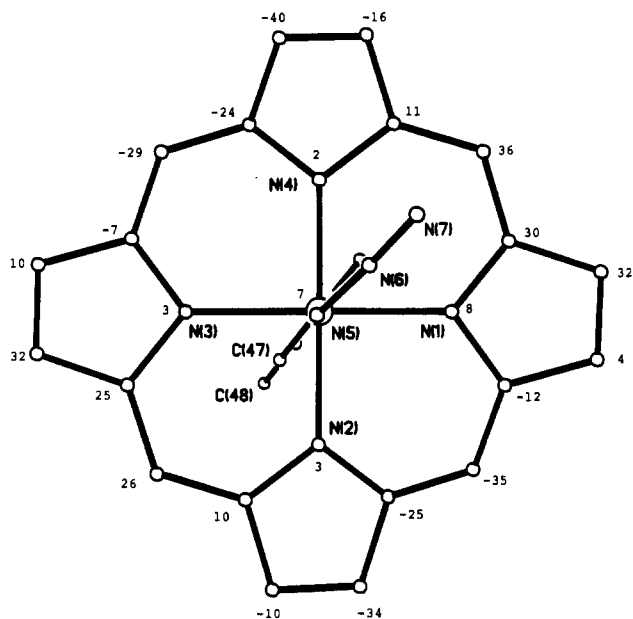
Figure 6. Diagram of the 24-atom porphyrin core in Fe(TPP)(1-MeIm)-N_3 (**4**) showing displacements (in units of 0.01 Å) of each atom from the mean plane of the core.
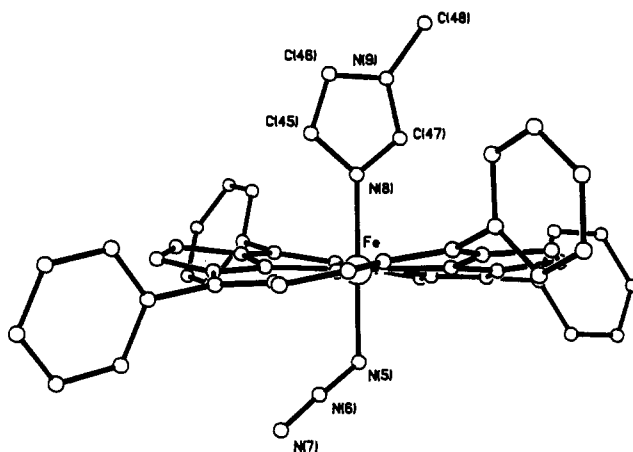
Figure 7. Side-on view of Fe(TPP)(1-MeIm)N_3 (**4**), showing the axial ligands and porphyrin core ruffling. The imidazole ligand is symmetrically located with respect to the mean plane of the core with $\alpha \approx 0°$ and $\beta \approx \gamma$.

2.09 μ_B at 77 K to 2.33 μ_B at 297 K. We found that Fe(TPP)(1,2-Me$_2$Im)N_3 behaves similarly, with μ_{eff} ranging from 2.03 μ_B at 77 K to 2.41 μ_B at 273 K. The dependence of μ_{eff} on temperature as well as the greater than spin-only value is fully expected[11] for a doublet ground state in a nearly octahedral environment (^2T term). Spin–orbit interactions split the ground state so that the Curie Law fails and μ_{eff} depends on temperature.

The structural details for **3** are provided in Figures 2–4 and Tables 1–3 and 8. The porphyrin core is somewhat domed, with the root-mean-square displacement from the mean plane of the 24 atom core (P_{core}) being 0.073 Å. The iron is displaced 0.510 Å from P_{core} and 0.457 Å from the plane of the four pyrrole nitrogens (P_N); the difference of 0.053 Å between these values is a measure of the extent of doming of the core away from the metal. Also relevant in this context are the N(1)–Fe–N(3) and N(2)–Fe–N(4) bond angles, which are 24 and 27°, respectively, from being linear. The out-of-plane displacement of the metal is similar to that found in other structures of high-spin five-coordinate Fe(III) porphyrins.[12–14] The average Fe–N bond

(11) (a) Figgis, B. N. *Introduction to Ligand Fields*; Interscience Publishers: New York, 1966; Chapter 10. (b) Drago, R. S. *Physical Methods for Chemists*; Saunders College Publishing: New York, 1992; Chapter 11.

Table 4. Selected Atomic Coordinates ($\times 10^4$) and Isotropic Thermal Parameters (Å$^2 \times 10^3$) for **4**

	x	y	z	U_{eq}
Fe	3626(1)	1966(1)	1137(1)	50(1)
N(1)	2574(4)	2156(2)	1845(4)	52(2)
N(2)	4479(4)	2648(2)	1614(3)	53(2)
N(3)	4687(4)	1784(2)	412(3)	50(2)
N(4)	2743(4)	1305(2)	611(3)	48(2)
N(5)	4525(4)	1558(2)	2194(4)	60(3)
N(6)	4146(5)	1251(3)	2643(5)	74(3)
N(7)	3834(7)	938(3)	3074(6)	121(4)
N(8)	2727(4)	2391(2)	43(4)	50(2)
N(9)	2262(5)	2991(2)	-1105(4)	80(3)
C(1)	2526(5)	2651(3)	2300(5)	64(3)
C(2)	3222(6)	3094(2)	2339(5)	59(3)
C(3)	4143(5)	3082(2)	2032(5)	60(3)
C(4)	4917(6)	3522(3)	2173(5)	77(4)
C(5)	5743(7)	3353(3)	1849(6)	84(4)
C(6)	5451(5)	2807(3)	1477(5)	68(3)
C(7)	6045(5)	2504(3)	998(6)	72(3)
C(8)	5702(5)	2019(3)	508(5)	57(3)
C(9)	6249(6)	1717(3)	-46(5)	71(3)
C(10)	5580(6)	1319(3)	-497(5)	66(3)
C(11)	4601(5)	1354(2)	-206(4)	52(3)
C(12)	3699(6)	994(2)	-509(2)	53(3)
C(13)	2833(5)	976(2)	-115(4)	51(3)
C(14)	1944(5)	599(3)	-376(5)	63(3)
C(15)	1346(5)	674(3)	215(5)	63(3)
C(16)	1832(5)	1113(2)	845(4)	54(3)
C(17)	1417(5)	1329(2)	1552(4)	54(3)
C(18)	1758(5)	1831(3)	1994(5)	58(3)
C(19)	1227(6)	2112(3)	2602(5)	77(4)
C(20)	1691(6)	2618(3)	2776(5)	80(4)
C(45)	1642(6)	2353(3)	-393(5)	76(4)
C(46)	1343(6)	2718(3)	-1087(6)	83(3)
C(47)	3068(6)	2774(3)	-419(5)	74(3)
C(48)	2338(7)	3440(4)	-1786(7)	142(5)

Table 5. Selected Bond Lengths (Å) and Bond Angles (deg) for **4**

Bond Lengths			
Fe–N(1)	1.978(6)	Fe–N(2)	1.992(4)
Fe–N(3)	1.999(5)	Fe–N(4)	1.983(4)
Fe–N(5)	1.931(5)	Fe–N(8)	1.987(5)
N(5)–N(6)	1.189(10)	N(6)–N(7)	1.134(12)
N(8)–C(45)	1.353(9)	N(8)–C(47)	1.299(10)
N(9)–C(46)	1.352(10)	N(9)–C(47)	1.331(8)
N(9)–C(48)	1.508(12)	C(45)–C(46)	1.329(11)

Bond Angles			
N(1)–Fe–N(2)	90.2(2)	N(1)–Fe–N(3)	179.2(2)
N(2)–Fe–N(3)	89.4(2)	N(1)–Fe–N(4)	90.0(2)
N(2)–Fe–N(4)	177.5(2)	N(3)–Fe–N(4)	90.4(2)
N(1)–Fe–N(5)	91.5(2)	N(2)–Fe–N(5)	90.1(2)
N(3)–Fe–N(5)	89.2(2)	N(4)–Fe–N(5)	92.4(2)
N(1)–Fe–N(8)	89.4(2)	N(2)–Fe–N(8)	89.3(2)
N(3)–Fe–N(8)	89.9(2)	N(4)–Fe–N(8)	88.3(2)
N(5)–Fe–N(8)	178.9(3)	Fe–N(5)–N(6)	122.3(5)
N(5)–N(6)–N(7)	176.1(8)	Fe–N(8)–C(45)	128.9(5)
Fe–N(8)–C(47)	126.8(4)	C(45)–N(8)–C(47)	104.2(5)
N(8)–C(45)–C(46)	110.7(7)	C(45)–C(46)–N(9)	106.4(6)
C(46)–N(9)–C(47)	106.0(6)	N(8)–C(47)–N(9)	112.6(6)
C(46)–N(9)–C(48)	126.0(6)	C(47)–N(9)–C(48)	128.0(6)

length to the pyrrole nitrogens (N_p) is 2.066 (3) Å and the dihedral angles between the phenyl rings and P_{core} in **3** are 67.4, 74.6, 72.8, and 85.3°. The Fe–N(5)–N(6) bond angle of 121.8° indicates sp^2 hybridization on the azide N(5) nitrogen, as expected. Figure 3 shows that the azide ligand in **3** is linear and does not eclipse a Fe–N_p bond axis, but rather is offset by the angle ϕ = 31.8(3)°. More precisely, ϕ is the dihedral angle between the planes defined by N(3)–Fe–N(5) and Fe–N(5)–N(6) (i.e., the N(3)–Fe–N(5)–N(6) torsion angle).

(12) Scheidt, W. R. *Acc. Chem. Res.* **1977**, *10*, 339.
(13) Scheidt, W. R.; Reed, C. A. *Chem. Rev.* **1981**, *81*, 543.
(14) (a) Fleischer, E. B.; Srivastava, T. S. *J. Am. Chem. Soc.* **1969**, *91*, 2403. (b) Hatano, K.; Scheidt, W. R. *Inorg. Chem.* **1979**, *18*, 877. (c) Anzai, K.; Hatano, K.; Lee, Y. J.; Scheidt, W. R. *Inorg. Chem.* **1981**, *20*, 2337.
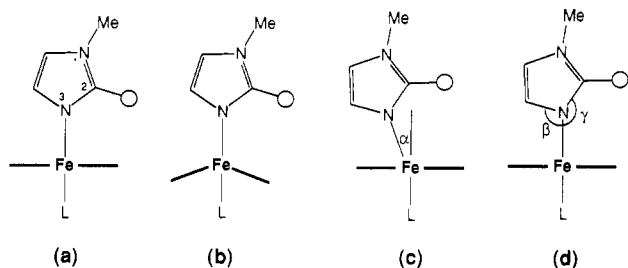
Figure 8. Model of a six-coordinate iron porphyrin with a 2-substituted imidazole ligand. The steric demands of the 2-substituent produce (a) no effect, (b) porphyrin core doming, (c) tilting of the imidazole, and (d) tipping of the imidazole.
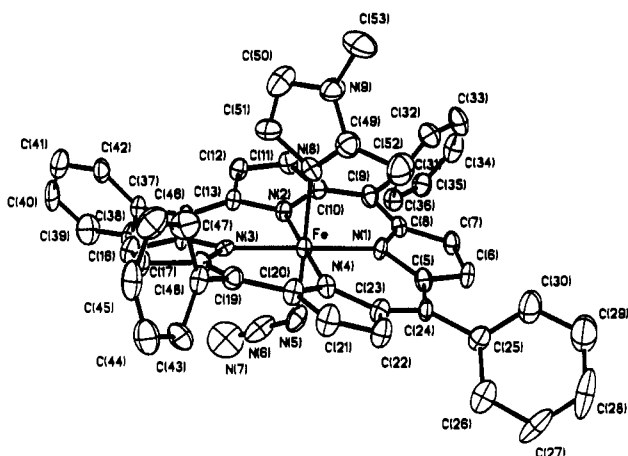
Figure 9. ORTEP diagram of Fe(TPP)(1,2-Me₂Im)N₃ (**5**). Probability surfaces are shown at 30%.
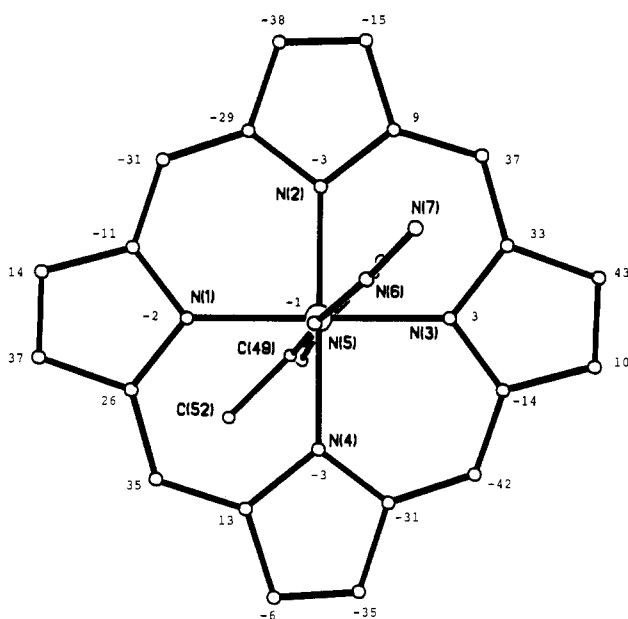
Figure 10. Diagram of the 24-atom porphyrin core in Fe(TPP)(1,2-Me₂Im)N₃ (**5**) showing displacements (in units of 0.01 Å) of each atom from the mean plane of the core.

Interestingly, during our studies it was found that **3** can also crystallize in the monoclinic system. The structure reported in Figures 2–4 was obtained subsequent to an analysis of another crystal, which was grown in a similar but independent experiment. The initial crystal was monoclinic with space group *Pc*. Refinement to R_w = 0.056 proceeded easily once it was realized that the Fe–N₃ unit was 2-fold disordered, with refined site occupancy factors of 0.78 and 0.22 for the two orientations. The major (78%) structure is very similar to that found in the triclinic crystal (Figures 2–4) with a Fe–N(5) bond length of 1.948(7) Å. The minor (22%) structure has Fe–N(5) = 1.909(24) Å with the
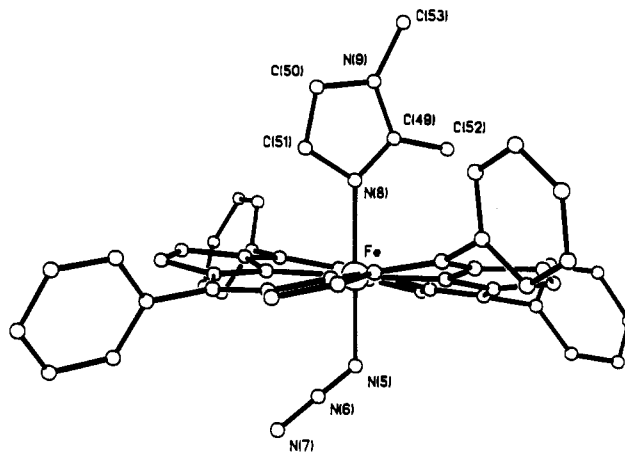
Figure 11. Side-on view of Fe(TPP)(1,2-Me₂Im)N₃ (**5**), showing the axial ligands and porphyrin core ruffling. The imidazole ligand is not tilted ($\alpha \approx 0°$) but is tipped such that $\beta < \gamma$ by 15°.

Table 6. Selected Atomic Coordinates (×10⁴) and Isotropic Thermal Parameters (Å² × 10³) for **5**

	x	y	z	U_{eq}
Fe	3548(1)	1970(1)	6209(1)	33(1)
N(1)	4603(6)	1778(3)	5493(5)	34(3)
N(2)	2655(6)	1333(3)	5638(5)	36(3)
N(3)	2500(5)	2154(3)	6939(5)	32(3)
N(4)	4424(6)	2618(3)	6762(5)	39(3)
N(5)	4353(6)	1521(3)	7225(7)	58(4)
N(6)	3951(7)	1236(4)	7648(8)	79(5)
N(7)	3576(13)	913(7)	8064(12)	148(6)
N(8)	2674(7)	2457(4)	5139(6)	46(4)
N(9)	2039(8)	3065(4)	4050(7)	60(4)
C(5)	5633(8)	1972(4)	5653(7)	41(4)
C(6)	6183(8)	1658(4)	5087(8)	48(5)
C(7)	5517(8)	1296(4)	4598(7)	44(4)
C(8)	4537(7)	1368(4)	4844(6)	37(4)
C(9)	3647(8)	1029(4)	4511(7)	43(4)
C(10)	2763(7)	1013(4)	4870(7)	39(4)
C(11)	1887(8)	644(4)	4600(7)	43(4)
C(12)	1265(8)	719(4)	5193(7)	44(4)
C(13)	1732(7)	1139(4)	5857(7)	38(4)
C(14)	1326(7)	1337(4)	6587(7)	34(4)
C(15)	1691(7)	1810(4)	7080(7)	38(4)
C(16)	1216(8)	2081(4)	7760(8)	53(5)
C(17)	1677(8)	2588(4)	7959(7)	49(4)
C(18)	7480(7)	2366(4)	2452(7)	34(4)
C(19)	8168(7)	1924(4)	2523(7)	42(4)
C(20)	9110(8)	1943(4)	2228(7)	42(4)
C(21)	4930(9)	3465(4)	7438(8)	55(5)
C(22)	5754(9)	3281(4)	7140(7)	50(5)
C(23)	5452(7)	2752(4)	6707(7)	45(4)
C(24)	6050(7)	2423(4)	6217(7)	38(4)
C(49)	2912(10)	2859(5)	4628(9)	60(6)
C(50)	1178(10)	2773(6)	4228(11)	80(6)
C(51)	1559(10)	2409(5)	4902(8)	60(5)
C(52)	3951(10)	3051(5)	4621(9)	84(6)
C(53)	1921(11)	3530(6)	3390(9)	98(7)

azide ligand situated on the side of the porphyrin opposite to that in the major form. Throughout the remainder of this paper, all analysis and discussion of the structural features of **3** refer to the ordered triclinic form.

The structural details for Fe(TPP)(1-MeIm)N₃ (**4**) are given in Figures 5–7 and Tables 1, 4, 5, and 8. As is commonly seen[6,8,15] with six-coordinate metalloporphyrins, the core displays approximate S_4 ruffling with the methine carbons alternating above and below the mean plane of the core with an average absolute displacement of 0.315 Å. The rms displacement for the 24 atom core is 0.227 Å. The iron atom projects slightly toward the azide, being 0.067 and 0.027 Å from P_{core} and P_N, respectively. The

(15) Munro, O. Q.; Bradley, J. C.; Hancock, R. D.; Marques, H. M.; Marsicano, F.; Wade, P. W. *J. Am. Chem. Soc.* **1992**, *114*, 7218.

Table 7. Selected Bond Lengths (Å) and Bond Angles (deg) for **5**

				Bond Lengths			
Fe–N(1)	1.977(8)	N(8)–C(51)	1.417(16)	Fe–N(2)	1.984(7)	N(8)–C(49)	1.308(16)
Fe–N(3)	1.980(8)	N(9)–C(50)	1.402(18)	Fe–N(4)	1.989(7)	N(9)–C(49)	1.341(15)
Fe–N(5)	1.934(8)	N(9)–C(53)	1.463(16)	Fe–N(8)	2.070(8)	C(50)–C(51)	1.326(18)
N(5)–N(6)	1.136(15)	C(49)–C(52)	1.435(19)	N(6)–N(7)	1.165(21)		

				Bond Angles			
N(1)–Fe–N(2)	90.4(3)	N(5)–Fe–N(8)	179.0(4)	N(1)–Fe–N(3)	179.2(3)	Fe–N(5)–N(6)	121.6(7)
N(2)–Fe–N(3)	89.5(3)	N(5)–N(6)–N(7)	175.3(14)	N(1)–Fe–N(4)	89.8(3)	Fe–N(8)–C(51)	119.1(8)
N(2)–Fe–N(4)	178.8(3)	Fe–N(8)–C(49)	133.8(8)	N(3)–Fe–N(4)	90.3(3)	C(49)–N(8)–C(51)	106.8(9)
N(1)–Fe–N(5)	87.8(4)	N(8)–C(51)–C(50)	108.0(11)	N(2)–Fe–N(5)	92.9(3)	C(51)–C(50)–N(9)	107.3(11)
N(3)–Fe–N(5)	91.4(4)	C(49)–N(9)–C(50)	107.0(10)	N(4)–Fe–N(5)	88.3(3)	N(8)–C(49)–N(9)	110.8(11)
N(1)–Fe–N(8)	93.1(3)	C(50)–N(9)–C(53)	123.0(10)	N(2)–Fe–N(8)	87.5(3)	C(49)–N(9)–C(53)	129.8(11)
N(3)–Fe–N(8)	87.6(3)	N(8)–C(49)–C(52)	126.6(11)	N(4)–Fe–N(8)	91.4(3)	N(9)–C(49)–C(52)	122.5(12)

Table 8. Structural Parameters for Heme Protein Models[a]

compound	Fe–N_p	Fe–N_{Im}	Fe–N_3 or Fe–O_2	Fe–P_{core}	Fe–P_N	ϕ_{Im}	ref
Fe(TPP)N₃ (**3**)	2.066(3)		1.953(5)	0.510(3)[b]	0.457(3)[b]		c
Fe(TPP)(1,2-Me₂Im)N₃ (**5**)	1.983(8)	2.070(8)	1.934(8)	-0.008(8)	0.004(8)	43.4(12)	c
Fe(TPP)(1-MeIm)N₃ (**4**)	1.988(5)	1.987(5)	1.931(5)	0.067(6)	0.027(5)	38.3(6)	c
Fe(TPP)(py)N₃	1.989(6)	2.089(6)[d]	1.925(7)	0.035		40[d]	6
Fe(TPP)(2-MeIm)	2.086(4)	2.161(5)		-0.55	-0.42	7.4	18
Fe(TpivPP)(2-MeIm)	2.071(5)	2.095(6)		-0.426	-0.399	22.8	3
Fe(TpivPP)(2-MeIm)O₂ (**2**)	1.997(4)	2.107(4)	1.898(7)	-0.110	-0.086	22.2	3
Fe(TpivPP)(1-MeIm)O₂ (**1**)	1.978(10)	2.068(18)	1.745(18)	0.015	0.03	20	2
T-α-oxy hemoglobin[e]	2.03(4)	2.2(1)	1.82(4)	-0.37(4)	-0.18(5)	11	1
R-oxy hemoglobin[f]	1.99(5)	1.94(9)	1.66(8)	-0.16(8)	-0.12(8)	11	1

[a] Fe–N_p is the average bond length (Å) to the pyrrole nitrogens; Fe–N_{Im} is the bond length (Å) to the imidazole nitrogen; P_{core} is the plane of the 24 atom porphyrin core; P_N is the plane of the four pyrrole nitrogens; ϕ_{Im} is the angle (deg) between an N_p–Fe–N_p bond axis and the imidazole plane. [b] A positive value means the metal is displaced toward the N_3 (or O_2) and away from an imidazole (if present). [c] This work. [d] Refers to the pyridine ligand. [e] Parameters are an average of those for α subunits. [f] For α subunits.

average Fe–N_p bond length in **4** is 1.988(5) Å, a value 0.078 Å less than that in **3**; this decrease in Fe–N_p is typical of a high-spin to low-spin conversion with iron(III) porphyrins.[8] In comparison to **3**, the Fe–N_3 bond length in **4** is very slightly decreased (by 0.022(10) Å) and the Fe–N(5)–N(6) bond angle is unchanged (122.3° in **4**). The dihedral angles between P_{core} and the phenyl rings are 67.1, 72.8, 75.8, and 78.4°. The imidazole is highly planar with the rms displacement of the five atom ring being 0.010 Å. The dihedral angle ϕ between the imidazole plane and the plane defined by [N(2),Fe,N(4),N(8)] is 38°, which means that the projection of the former intersects the N(2)–Fe–N(4) bond axis at this angle. Similarly, the azide ligand almost exactly bisects the Fe–N(4) and Fe–N(1) axes with $\phi = 45°$.

Figure 8 illustrates possible orientations of an imidazole ligand in a six-coordinate metalloporphyrin. The "ideal" structure (Figure 8a) has the metal in plane with the imidazole ligand coordinated in a symmetrical fashion. Any steric interactions from a 2-substituent can be alleviated by doming of the porphyrin core (8b) and tilting ($\alpha \neq 0$; Figure 8c) or tipping ($\beta \neq \gamma$; Figure 8d) of the imidazole. Of course, in **4** the 2-substituent is hydrogen and there appears to be no significant sterically-induced structural features. Figure 8a is the best representation of **4**. The N(5)–Fe–N(8) axis is linear (179°; $\alpha \approx 0°$), the bond angles N(i)–Fe–N(5) and N(i)–Fe–N(8) ($i = 1–4$) are all close to 90°, and the dihedral angles between P_{core} and the imidazole and Fe–N_3 planes are 89.4 and 89.5°, respectively. The angles β and γ (Figure 8d) are 129 and 127° for **4**, indicating no significant tipping of the ligand. The structure of **4** is analogous in many ways to that of Fe(TPP)(py)N₃ (**6**), which was reported by Scheidt et al.[6] Complexes **4** and **6** have similar porphyrin core S_4 ruffling and essentially the same Fe–N_3 bond length. The pyridine ligand in **6** is more sterically demanding than the 1-MeIm in **4** and this is reflected by a long Fe–Py bond length (2.089 Å). The pyridine is not markedly tilted ($\alpha \approx 0°$) or tipped ($\beta \approx \gamma$).

Figures 9–11 and Tables 1 and 6–8 give the relevant structural features for Fe(TPP)(1,2-Me₂Im)N₃ (**5**). The porphyrin core in **5** is ruffled much as seen in **4**, with an average absolute displacement of the methine carbons of 0.36 Å. The rms displacement for the entire core is 0.258 Å. The iron atom is

located in P_{core} and P_N with an average Fe–N_p bond length of 1.983(8) Å. The Fe–N_3 bond length and Fe–N(5)–N(6) bond angle is essentially identical to that in **4**. The dihedral angles between P_{core} and the phenyl rings are 58.8, 65.4, 70.8, and 72.7°. The five-atom imidazole ring is planar with an rms displacement of 0.017 Å. The projection of the imidazole plane forms an angle ϕ of 43° with the N(2)–Fe–N(4) bond axis while the azide ligand projection is 41° from the Fe–N(3) bond axis. As with **4**, complex **5** has a linear N(5)–Fe–N(8) bond axis (179°), bond angles N(i)–Fe–N(5) and N(i)–Fe–N(8) ($i = 1–4$) that are close to 90°, and dihedral angles between P_{core} and the imidazole and Fe–N_3 planes that are also nearly 90° (88.2 and 89.7°, respectively).

There are, however, substantial differences between the structures of **4** and **5** which can reasonably be ascribed to the presence of the sterically demanding 2-Me substituent in **5**. While the Fe–N_3 and Fe–N_p bond lengths are the same in **4** and **5**, the iron–imidazole bond, Fe–N_{Im}, is longer in **5** by 0.083 Å and the metal is in the P_{core} plane in **5** while in **4** it is 0.067 Å from P_{core} toward the azide. A visual comparison of Figures 7 and 11 shows an obvious tipping of the imidazole in **5**, which reduces contacts involving the 2-Me group. The tipping (Figure 8d) is almost 15°, as measured by the angles β (119.1(8)°) and γ (133.8(8)°), and is clearly sterically induced since it is absent in **4**. It is relevant to note that such tipping ($\beta < \gamma$) has previously been shown to occur in [Fe(TPP)(RIm)₂]ClO₄[16] and Fe(TpivPP)(RIm)O₂[2,3] when RIm is changed from 1-MeIm to 2-MeIm.

Table 8 gives a summary of structural information for a variety of relevant complexes. The picket fence complexes **1** and **2** are generally considered good models for R- and T-state HbO₂.[2,3] In **2**, the 2-MeIm ligand is tilted by $\alpha = 7°$ (Figure 8c) *and* tipped (Figure 8d) with $\beta < \gamma$ by 11.7(11)°. In going from **2** to **1**, the principal structural changes are (1) some movement of the metal in the direction of O₂, (2) a large decrease in the Fe–O₂ bond length, (3) a slight decrease in bond distances Fe–N_{Im} and Fe–N_p, and (4) untilting and untipping of the imidazole to give the symmetrical structure in Figure 8a. The azide complexes **4** and

(16) Scheidt, W. R.; Kirner, J. F.; Hoard, J. L.; Reed, C. A. *J. Am. Chem. Soc.* **1987**, *109*, 1963.

5 show some significant differences in comparison with their picket fence analogues. The imidazole in **5** is tipped by 15° but is *not* tilted off-axis as is **2**. Just as with **2** → **1**, the conversion **5** → **4** produces some movement of the metal in the direction of the small ligand (N₃) and untipping of the imidazole. However, **5** → **4** does *not* lead to a decrease in the Fe–N₃ bond length and *does* produce a large decrease of the Fe–N$_{Im}$ distance. In neither the oxygen nor the azide complexes is the orientation angle[17,18] ϕ altered substantially by the steric demands of the 2-Me substituent.

In hemoglobin, the evidence suggests that the T → R transformation in HbO₂ is accompanied by (1) movement of the metal in the direction of O₂, (2) a decrease in the Fe–N$_{Im}$ and (possibly) the Fe–O₂ bond lengths, (3) an untilting of the proximal imidazole from its off-axis position in T-HbO₂, and (4) no change in the orientation angle ϕ. One would hardly expect that the azide complexes **4** and **5** would follow in detail the changes occurring in the protein T → R switch, but it can be seen that the model complexes are successful in mimicking some aspects of the bond length and angle variations.

Supplementary Material Available: Complete atom coordinates, thermal parameters, bond lengths, bond angles, and torsion angles for complexes **3–5** (31 pages). Ordering information is given on any current masthead page.

(17) (a) Scheidt, W. R.; Chipman, D. M. *J. Am. Chem. Soc.* **1986**, *108*, 1163. (b) Uemori, Y.; Miyakawa, H.; Kyuno, E. *Inorg. Chem.* **1988**, *27*, 377. (c) Safo, M. K.; Scheidt, W. R.; Gupta, G. P. *Inorg. Chem.* **1990**, *29*, 626. (d) Safo, M. K.; Gupta, G. P.; Walker, F. A.; Scheidt, W. R. *J. Am. Chem. Soc.* **1991**, *113*, 5497. (e) Hatano, K.; Safo, M. K.; Walker, F. A.; Scheidt, W. R. *Inorg. Chem.* **1991**, *30*, 1643. (f) Munro, O. Q.; Bradley, J. C.; Hancock, R. D.; Marques, H. M.; Marsicano, F.; Wade, P. W. *J. Am. Chem. Soc.* **1992**, *114*, 7218.

(18) Hoard, J. L. In *Porphyrins and Metalloporphyrins*; Smith, K. M., Ed.; Elsevier Scientific Publishing Co.: New York, 1975; Chapter 8.